ChemistrySelect

Research Article
doi.org/10.1002/slct.202202232

Chemistry Europe
European Chemical Societies Publishing

www.chemistryselect.org

Inorganic Chemistry

Synthesis and Properties of Bis(nitrocarbamoylethyl) Nitramine - A New Energetic Open-Chain Nitrocarbamate

Thomas M. Klapötke,* Burkhard Krumm,* Jasmin T. Lechner, and Christian Riedelsheimer[a]

The nitrocarbamate derivative of the well-known and intensively investigated nitro ester DINA was prepared and studied. Starting with bis(hydroxyethyl) nitramine obtained from DINA, the corresponding carbamate was obtained by treatment with chlorosulfonyl isocyanate (CSI). Using fuming nitric acid only as nitration reagent, the target compound bis(nitrocarbamoylethyl) nitramine was synthesized. Furthermore, a route to the salt bis(nitrocarbamoylethyl)ammonium nitrate by a simple two step synthesis starting from diethanolamine was revealed. The compounds were fully characterized by NMR spectroscopy, X-ray diffraction, differential thermal analysis, vibrational analysis and elemental analysis. The sensitivities towards impact and friction of the energetic compounds were measured, as well as their energetic properties determined by using the energies of formation, calculated on the CBS4-M level of theory, with the EXPLO5 computer code.

Introduction

The discovery of nitroglycerine (NG) and nitrocellulose (NC) ultimately formed the foundation for modern propellants.[1–3] The strategy for developing new energetic nitro esters changed slightly due to the need to increase the energy levels of the existing propellant mixtures. Therefore, other nitro esters were added to nitroglycerine to lower its freezing point while increasing the impact and friction sensitivity values, leading to overall safer handling.[1,3–4] Ethylene glycol dinitrate (EGDN) for example is a plasticizer used as such an additive. While this plasticizer appears to have similar building blocks like NG, their properties differ.

EGDN (7456 m s^{-1}) has a lower detonation velocity value than NG (7694 m s^{-1}), but is generally more stable and less sensitive towards impact, shown in Figure 1.[5] Although EGDN has a higher volatility, it has a good oxygen balance (OB), which is defined as the relative amount of oxygen excess (+) or deficit (−) remaining after combustion of the energetic material. Nitroglycerine, on the other hand, is an explosive with a positive OB value ($\Omega_{CO2} = +3.5\,\%$). Accordingly, it seemed reasonable to combine NG with oxygen-deficient explosives such as nitrocellulose to obtain a more balanced OB value.[1,3–4]

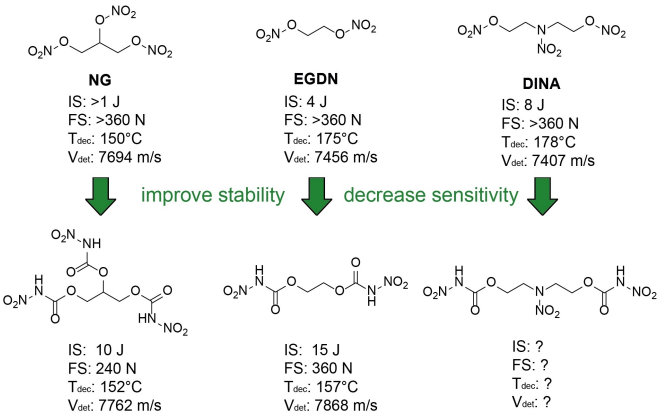

Figure 1. Nitro esters NG, EGDN and DINA with their properties in comparison to their corresponding nitrocarbamates (values are calculated with the newest EXPLO5 version: V6.06.01).[5]

In the 1940s, the nitroxyethylnitramine (NENA) plasticizers were described, which are characterized by containing both nitro ester and nitramine functionalities, making them some of the most powerful explosives available.[6] Dinitrooxyethylnitramine dinitrate (DINA), shown in Figure 1, has a similar explosive performance to RDX and is used as a substitute for NG due to its higher energy, larger specific volume, lower combustion temperature, and good thermal stability.[7] Moreover, DINA is used as an ingredient in the production of double base propellant to improve mechanical properties at low temperatures,[8–11] and has a conveniently low melting point that enables melt casting.[4]

Unfortunately, the advantageous and powerful properties of nitro esters are not without several drawbacks. Not only they are more sensitive than their *C*-nitro counterparts and often

[a] *Prof. Dr. T. M. Klapötke, Dr. B. Krumm, Jasmin T. Lechner, C. Riedelsheimer*
Department of Chemistry,
Ludwig Maximilian University of Munich
Butenandtstr. 5–13 (D),
81377 Munich (Germany)
E-mail: tmk@cup.uni-muenchen.de
bkr@cup.uni-muenchen.de
Homepage: http://www.hedm.cup.uni-muenchen.de

Supporting information for this article is available on the WWW under https://doi.org/10.1002/slct.202202232

undergo thermal decomposition, they also lack in chemical stability.[2] Nitro esters hydrolyze in the presence of acids or bases, and are not resistant to prolonged exposure to water or moisture. Given these disadvantages, long-term storage of these substances is difficult. However, the amount of autocatalytic decomposition can be limited by adding stabilizers to the propellant composition, which trap the nitrous decomposition products and convert them into stable compounds, ultimately delaying the decomposition process.[12]

Considering the disadvantages associated with nitro esters, there is an obvious need to increase the stability of propellants, therefore the group of nitrocarbamates will be discussed in more detail below. The carbamate functionality exhibits characteristic properties of amides and esters as it contains a carbonyl function directly linked to an amino function, which can be nitrated to form *N*-nitrocarbamates.[11,13] These were first reported in 1895[14] and more thoroughly investigated by us in 2016, by converting alcohols (some well-known precursors of their nitro esters), into carbamates and further into nitrocarbamates.[15] Thereby, the thermal stability as well as sensitivity values towards impact and friction are increased. In addition, the new nitrocarbamates have good physical properties and are more stable to acid hydrolysis due to the functionality of the carbonyl group.[15–16] The structure of the corresponding nitrocarbamates of NG and EGDN with their properties are shown in Figure 1. However, the oxygen balance often decreases, but the nitrogen content increases, which can result in a higher detonation performance as in the case of the corresponding nitrocarbamates of NG and EGDN.[15] Therefore, in this work, the preparation of the corresponding nitrocarbamate of DINA was attempted and the physical and energetic properties have been compared with the nitro esters DINA and EGDN.

Results and Discussion

Synthesis

The starting material diethanolamine (DEA) was converted into the corresponding carbamate, bis(carbamoylethyl) amine (**1**) by reaction with chlorosulfonyl isocyanate (CSI) according to the established method.[13]

For the nitration of all three amino groups of **1** various reagents were tested. Harsh conditions such as mixtures of nitric acid with oleum or acetic acid anhydride[17] failed due to decomposition. Milder conditions such as the combination of ammonium nitrate with trifluoroacetic acid[18] or N_2O_5[19] were also not successful. Treatment with fuming nitric acid resulted in formation of the nitrate salt **2** (Scheme 1). While the carbamate moiety is nitrated, the secondary nitrogen is protonated only.

Based on this observation, an approach via the known nitramine bis(hydroxyethyl) nitramine was pursued. This potential precursor is accessible from the corresponding nitro ester bis(nitratoethyl) nitramine (**3**, DINA, Figure 1).

DINA is usually synthesized from diethanolamine by employing mixtures of HNO_3/MgO[10] or HNO_3/Ac_2O.[17,20–21] For this purpose, MgO or Ac_2O are used as dehydrating agents.[17] Starting from the HNO_3/MgO approach[10], diethanolamine is first converted into diethanolamine dinitrate (DIA) via *O*-nitration[2,22] by heating and addition of NaCl as a catalyst. Further *N*-nitration[23] leads to the formation of DINA.

This reaction has several disadvantages, requiring both a catalyst[20] and heat source to form the product. Moreover, the product could only be obtained with low yield and poor purity. The sticky consistency can be attributed to the undesirable formation of $Mg(OH)_2$.[17] The two-step synthesis also leads to the formation of the intermediate DIA. DIA was shown to have a lower thermal stability than DINA[24], therefore a potential risk and its accumulation should be avoided.[17]

The traditional HNO_3/Ac_2O method[21,24] was optimized in 2019.[17] Here, the starting material diethanolamine is replaced by diethanolamine hydrochloride (DEAHC), which previously served as a catalyst for the synthesis of DEA to DINA.[20–21] This chloride salt is the reagent of choice for the nitration to DINA (**3**) with minimized safety concerns.

This synthesis was pursued and switched from continuous flow[17] to a conventional batch synthesis to test the efficiency and compare the two approaches. Care was taken to dose DEAHC and HNO_3 in a controlled manner. Considering that a higher molar ratio of Ac_2O to reactant benefits the overall process by improving the safety and yield of the synthesis, excess of Ac_2O was applied, which is in accordance with the molar ratio reported in the continuous flow procedure.[17] The nitration was carried out without the addition of heat, in fact, cooling was only applied when the reactants were added (Scheme 2). The batch synthesis was successfully carried out as DINA (**3**) was obtained with high purity and yield.

Further controlled hydrolysis of **3** to the desired nitramine **4** was achieved *via* a combination of known procedures.[25–26] DINA was first refluxed with formic acid which reduced exclusively the *O*-nitratomethyl units back to the hydroxymethyl moiety. After removal of formic acid, additional refluxing in methanol is required. Isolation and purification of **4** is performed by column chromatography. Storage of **4** is required at low temperatures.

Now, with this precursor available, a conversion to the corresponding bis(carbamoylethyl) nitramine (**5**) is performed

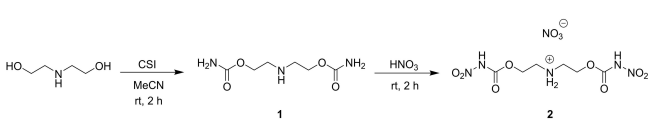

Scheme 1. Preparation and nitration of bis(carbamoylethyl) amine (**1**).

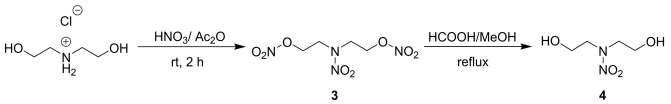

Scheme 2. Nitration to form DINA (**3**) and further hydrolysis to form bis(hydroxyethyl) nitramine (**4**).

as described earlier. Followed by nitration at 0 °C for one hour the desired nitrocarbamate bis(nitrocarbamoylethyl) nitramine (**6**) was obtained and isolated (Scheme 3).

NMR spectroscopy

All materials were characterized by $^{1}H/^{13}C$ NMR and nitro group containing compounds also by ^{14}N NMR spectroscopy in DMSO-D_6 as solvent (for assignments see Experimental Section). Additionally, the ^{15}N NMR spectrum of **6** was recorded in acetone-D_6 (Figure 2) and is discussed in more detail.

The four resonances, two nitro and two amine resonances, are observed in the typical regions around −35 and −200 ppm. The central nitro resonance at −29.7 ppm is split into a quintet ($^{3}J_{N,H}$ = 2.9 Hz) due to coupling with the two methylene groups attached to the nitramine unit. The terminal nitro groups resonate at −45.0 ppm as a singlet. The nitrocarbamate nitrogen resonance is detected at −189.4 ppm as a broadened dublet ($^{1}J_{N,H}$ = 89.9 Hz), whereas that of the central nitramine nitrogen is observed at −207.7 ppm as a singlet.

Single crystal analysis

A single-crystal X-ray diffraction analysis was performed for **2**, **5** and **6** (Table 1).

Bis(nitrocarbamoylethyl)ammonium nitrate (**2**) crystallizes in the triclinic space group of $P\bar{1}$ (Figure 3) with two molecules in its unit cell.

Bis(carbamoylethyl) nitramine (**5**) crystallizes in the monoclinic space group $C2/c$ with four molecules per unit cell (Figure 4).

Bis(nitrocarbamoylethyl) nitramine (**6**) crystallizes in the monoclinic space group $P2_1$ with one molecule per unit cell (Figure 5).

The bond lengths in the carbamate units of N1-C1 in **5** (1.325(3) Å) and N2−C1 in **6** (1.370(5) Å), differ by 0.045 Å. The longer bond of **6** is due to the electron withdrawing effect of the nitro group in **6**.

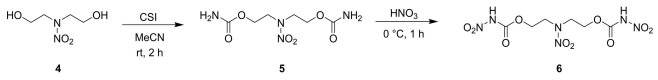

Scheme 3. Carbamoylation and nitration of **4** to form the nitrocarbamate **6**.

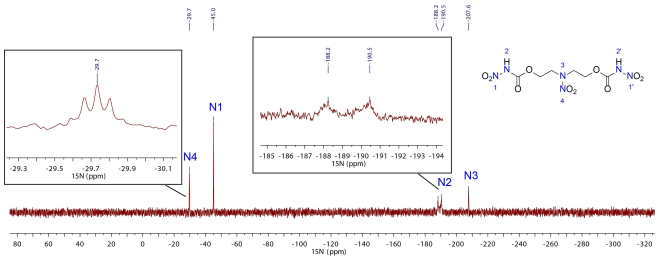

Figure 2. ^{15}N NMR spectrum of bis(nitrocarbamoylethyl) nitramine (**6**) in acetone-D_6.

Table 1. Crystallographic data of **2**, **5** and **6**.

	2	5	6
Formula	$C_6H_{12}N_6O_{11}$	$C_6H_{12}N_4O_6$	$C_6H_{10}N_6O_{10}$
FW [g mol^{-1}]	344.22	236.20	326.18
Crystal system	triclinic	monoclinic	monoclinic
Space group	*P*-1	*C*2/*c*	$P2_1$
Color/Habit	colorless block	colorless plate	colorless plate
Size [mm]	0.20x0.17x0.08	1.0x0.76x0.10	0.12x0.08x0.02
a [Å]	7.4011(5)	8.1385(15)	6.4019(6)
b [Å]	9.0114(6)	6.0196(11)	9.6138(9)
c [Å]	11.1321(7)	20.395(4)	10.1326(9)
α [°]	76.213(5)	90	90
β [°]	79.670(5)	98.973(16)	104.705(3)
γ [°]	66.974(6)	90	90
V [Å^3]	660.52(8)	986.9(3)	603.20(10)
Z	2	4	2
ρ_{calc} [g cm^{-3}]	1.731	1.590	1.796
μ [mm^{-1}]	0.167	0.142	0.17
F (000)	356	496	336
$\lambda_{MoK\alpha}$ [Å]	0.71073	0.71073	0.71073
T [K]	101	102	173
θ Min-Max [°]	1.89, 26.37	2.02, 26.4	2.97, 25.4
Dataset	−9≤9; −11≤11; −13≤13	−9≤10; −7≤7; −20≤25	−7≤7; −11≤0; −12≤0
Reflections coll.	9723	3050	37891
Independent refl.	1959	1181	1160
R_{int}	0.040	0.048	0.025
Parameters	256	98	200
*R*1 (obs)[a]	0.0778	0.0663	0.039
w*R*2 (all data)[b]	0.1156	0.1448	0.1017
S [c]	1.025	1.175	1.196
Resd. Dens. [e Å^{-3}]	−0.206, 0.343	−0.295, 0.315	−0.22, 0.27
Device type	Xcalibur, Sapphire 3	Xcalibur, Sapphire 3	D8 Venture
Solution	SHELXT 2018/2	SHELXT 2018/2	SHELXT 2018/2
Refinement	ShelXL 2018/3	ShelXL 2018/3	ShelXL 2018/3
Absorption corr.	multi-scan	multi-scan	multi-scan
CCDC	2169524	2169525	2169523

[a] $R1 = \Sigma||F0|-|Fc||/\Sigma|F0|$; [b] $wR2 = [\Sigma[w(F02-Fc2)2]/\Sigma[w(F0)2]]1/2$; $w = [\sigma c2(F02) + (xP)2 + yP]$-1 and $P = (F02 + 2Fc2)/3$; [c] $S = \{\Sigma[w(Fo2-Fc2)2]/(n-p)\}1/2$ (n = number of reflections; p = total number of parameters).

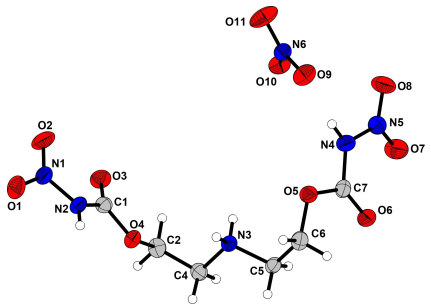

Figure 3. Molecular structure of **2**. Selected bond lengths (Å): N2-C1 1.384(3), N1-N2 1.370(3), O1-N1 1.222(3), N1-O2 1.217(3), N4-C7 1.385(3), N5-N4 1.374(3), O7-N5 1.211(3), O8-N5 1.222(3), N3-C4 1.490(3), N3-C5 1.491(3). Selected angles (°): O3-C1-N2 127.0(2), O6-C7-N4 127.6(2), O1-N1-N2-C1 158.5(2), O2-N1-N2-C1 −21.2(3), O7-N5-N4-C7 17.7(4), O8-N5-N4-C7 -161.9(2).

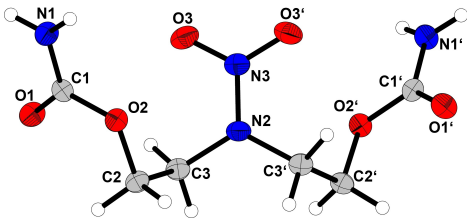

Figure 4. Molecular structure of **5**. Selected bond lengths (Å): N1-C1 1.325(3), N3-N2 1.338(4), O3-N3 1.241(2). Selected angles (°): O1-C1-N1 124.6(2), O3-N3-N2-C3 176.66(14).

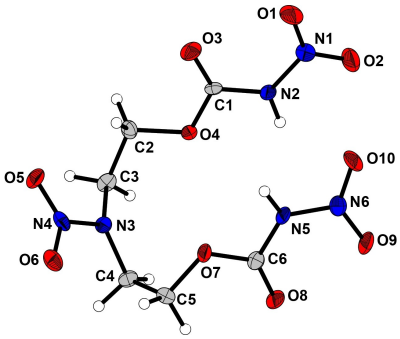

Figure 5. Molecular structure of **6**. Selected bond lengths (Å): N2-C1 1.370(6), N3-N4 1.358(6), N1-N2 1.386(6), O5-N4 1.237(6), N1-O1 1.201(7). Selected angles (°): O3-C1-N2 126.4(5),O8-C6-N5 126.9(5) O5-N4-N3-C3 −10.9(6), O1-N1-N2-C1 9.9(7), O9-N6-N5-C6 −11.8(7), O2-N1-N2-C1 −170.1(5), O10-N6-N5-C6 169.0(5), N1-N2-C1-O4 177.4(5).

The bond angles of magnetically equivalent atoms in the same substance may differ, thus the nitrocarbamates **2** and **6** will be discussed in more detail. For this purpose, the two oxygen atoms of the nitro group are distinguished, depending on which is closer to the corresponding carbonyl group. The torsion angles of the O-atom facing the carbonyl are −21.2(3)° for O2-N1-N2-C1 and 17.7(4)° for O7-N5-N4-C7. This results in a difference of 3.6°. The torsion angle of the oxygen atom farther from the carbonyl oxygen is 158.5(2)° for O1-N1-N2-C1 and −161.9(2)° for O8-N5-N4-C7. This results in an overall difference of 3.4°. Compound **6** shows the same trend, although the difference is much smaller compared to **2**. The oxygen atoms facing the carbonyl group show a difference of 1.9° (O1-N1-N2-C1 9.9(7)°, O9-N6-N5-C6 −11.8(7)°) and the oxygen atoms farther away from the carbonyl group showing a difference of 1.1° (O2-N1-N2-C1 −170.1(5)°, O10-N6-N5-C6 169.0(5)°).

A difference between the bond angles of carbamate **5** and nitrocarbamate **6** can also be observed. The O=C–N angles of **6** are 126.4(5)° for O3-C1-N2 and 126.9(5)° for O8-C6-N5, whereas that of **5** is 124.6(2)° for O1-C1-N1. The angles of **6** differ only slightly by 0.5°. However, the difference between **5** and **6** is in the range of 1.8-2.3°, indicating that the nitration of the carbamate strongly influences this angle.

Thermal analysis

A differential thermal analysis (DTA) study was performed for the thermal characterization of **1**, **2**, **3**, **5** and **6**. A heating rate of 5 °C per minute was used for this purpose. The endothermic and exothermic onset points are listed in Table 2 and plots of all DTAs can be found in the Supporting Information (Figure S18).

The endothermic signals of carbamates **1** and **5** (**1**: 207 °C, **5**: 175 °C) can be identified as melting points. The nitramine group of **5** evidently has a great influence on the melting point, since this functional group is the only structural difference between these two compounds. Decomposition occurs in both, which is reflected in the exothermic signals (**1**: 234 °C, **5**: 262 °C).

The salt **2** exhibits only an exothermic signal at 150 °C. However, it can be concluded, that the ionic compound undergoes a gradual exothermic conversion. The nitrocarbamate **6** shows both an endothermic (142 °C) and exothermic signal (153 °C). It can be assumed that the endothermic event initiates the exothermic decomposition of the structure. The DTA measurement shows that this compound does not decompose directly in one step, but first breaks down into smaller components. In summary, **2** and **6** have very similar thermal stability.

Sensitivities and energetic properties

The sensitivities towards impact (IS) and friction (FS) were determined and shown in Table 3.

The nitrocarbamates **2** (5 J) and **6** (6 J) have to be classified as impact sensitive. With an impact sensitivity of >40 J, substance **5** can be classified as insensitive.[24,27] Moreover, the friction sensitivity for all is >360 J, which implies insensitive towards friction.

The EXPLO5 code version 6.06.01[28] was used to calculate the energetic properties. The EXPLO5 calculations are performed based on the molecular formula, densities, and

Table 2. Endothermic[a] and exothermic[b] onset points of the DTA measurements.

	T_{endo} [a] [°C]	T_{exo} [b] [°C]
1	207	234
2	–	150
3	50	184
5	175	262
6	142	153

Table 3. Sensitivities towards friction and impact of **2**, **3**, **5**, and **6**.

	2	3	5	6
IS [J] [a]	5	8	>40	6
FS [N] [b]	>360	>360	>360	>360

[a] impact sensitivity according to the BAM drophammer (method 1 of 6); [b] friction sensitivity according to the BAM friction tester (method 1 of 6).

enthalpy of formation of the compounds. The comparison of **2** and **6** demonstrates how the properties affect the EXPLO5 calculation, since these two substances have a similar molecular formula, but differ in other characteristics. The enthalpy of formation of **6** (−683.3 kJ mol^{-1}) is greater than that of **2** (−1193.1 kJ mol^{-1}). At the same time the ionic compound **2** (1.68 g cm^{-3}) has a lower density than **6** (1.76 g cm^{-3}), which is why **2** (7251 m s^{-1}) has a lower detonation velocity value than **6** (7804 m s^{-1}).

The detonation velocity of **2** is lower compared to EGDN (7456 m s^{-1}) and DINA (7407 m s^{-1}). However, compound **6** was able to achieve the desired properties and has a higher detonation velocity compare to DINA or EGDN of 7804 m s^{-1}. The energetic properties are listed in Table 4.

Although EGDN and DINA (**3**) may have different structures and molecular formulas, the enthalpies of formation values are quite close (EGDN: −241.0 kJ mol^{-1}, DINA: −329.0 kJ mol^{-1}) and the densities are virtually identical (~ 1.48 g cm^{-3}). Thus, it is no surprise that the detonation velocities of EGDN and DINA are similar, although EGDN has an even higher detonation velocity than DINA owing to its higher enthalpy of formation.

Conclusion

In this work, the main goal was the synthesis and thorough characterization of the corresponding nitrocarbamate of the nitro ester DINA (dinitroxyethylnitramine dinitrate, **3**), bis(nitrocarbamoylethyl) nitramine (**6**).

In general, nitrocarbamates often show a higher thermal stability compared to the corresponding nitro esters.[15] Therefore, the thermal stability should be enhanced for **2** and **6** compared to DINA. However, this statement could not be confirmed by analytical measurements. On the contrary, DTA measurements revealed that DINA (184 °C) has indeed a higher thermal stability than its nitrocarbamate counterparts **2** (150 °C) and **6** (153 °C).

However, if the detonation parameters are compared, it can be seen that the higher nitrogen content and the better density of the nitrocarbamate **6** results in better detonation velocities compared with DINA (**3**). Further important calculated values of the nitrate salt **2** and nitrocarbamate **6** are compared to DINA with a bar chart in Figure 6.

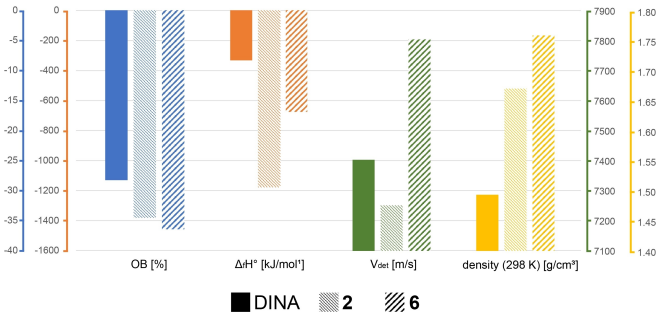

Figure 6. Bar chart comparing four different properties of DINA (**3**), **2** and **6**. OB: Oxygen balance (Ω = (xO-2yC-1/2zH)M/1600) [%]; $\Delta_f H°$: calculated (CBS-4 M) heat of formation [kJ mol^{-1}]; V_{det}: detonation velocity [m s^{-1}]; calc. density (298 K).

Experimental Section

CAUTION! All investigated compounds are potentially explosive energetic materials, which show partly increased sensitivities towards various stimuli (e.g. elevated temperatures, impact or friction). Therefore, proper security precautions (safety glass, face shield, earthed equipment and shoes, leather coat, Kevlar gloves, Kevlar sleeves, and ear plugs) have to be applied while synthesizing and handling the described compounds. The synthesis procedure and analytics can be found in the Supporting Information.

Table 4. Energetic properties of **2** and **6**, EGDN and DINA for comparison.[5]

	2	6	EGDN	DINA (3)
Formula	$C_6H_{12}N_6O_{11}$	$C_6H_{10}N_6O_{10}$	$C_2H_4N_2O_6$	$C_4H_8N_4O_8$
FW [g mol^{-1}]	344.19	326.18	152.06	240.13
ρ (298 K) [g cm^{-3}]	1.68[a]	1.76[a]	1.48	1.49
$T_{dec.}$ [°C][b]	150	153	175	184
$\Delta_f H°$ [kJ mol^{-1}][c]	−1193.1	−683.3	−241.0	−329.0
EXPLO5 V6.06.01				
P_{CJ} [GPa][d]	20.1	25.0	20.9	21.7
V_{det} [m s^{-1}][e]	7251	7804	7456	7407
$-\Delta_{ex}U°$ [kJ kg^{-1}][f]	3151	4071	6258	5156
T_{det} [K][g]	2403	2871	4371	3589
V_0 [L kg^{-1}][h]	782	743	810	833
Ω_{CO2} [%][i]	−32.5	−34.3	0	−26.6

[a] X-ray density converted to RT; [b] temperature of decomposition indicated by exothermic event according to DTA (onset temperatures at a heating rate of 5 °C min^{-1}); [c] calculated (CBS-4 M) heat of formation; [d] detonation pressure; [e] detonation velocity; [f] Energy of explosion; [g] Explosion temperature; [h] Assuming only gaseous products; [i] Oxygen balance (Ω = (xO-2yC-1/2zH)M/1600).

Acknowledgements

Financial support of this work is gratefully acknowledged from the Ludwig-Maximilians-Universität, the Office of Naval Research (ONR) under grant no. ONR N00014-19-1-2078 and the Strategic Environmental Research and Development Program (SERDP) under contract number W912HQ19 C0033. We also would like to thank Dr. Peter Mayer and Marcus Lommel M.Sc. for their help with X-ray measurements. Open Access funding enabled and organized by Projekt DEAL.

Conflict of Interest

The authors declare no conflict of interest.

Data Availability Statement

The data that support the findings of this study are available from the corresponding author upon reasonable request.

Keywords: Energetic materials · Nitrogen oxides · NMR spectroscopy · Propellants · X-ray single crystal analysis

[1] T. M. Klapötke, *Chemistry of High Energy Materials*, 5th., deGruyter, Berlin, **2019**.
[2] R. Boschan, R. T. Merrow, R. W. van Dolah, *Chem. Rev.* **1955**, *55*, 485–510.
[3] J. P. Agrawal, *High Energy Materials*, Wiley-VCH, Weinheim, **2010**.
[4] J. P. Agrawal, R. D. Hodgson, *Organic Chemistry of Explosives*, Wiley-VCH, Weinheim, **2007**.
[5] T. M. Klapötke, *Energetic Materials Encyclopedia*, 2nd Edition, DeGruyter, Berlin/Boston, **2021**.
[6] J. J. Sabatini, E. C. Johnson, *ACS Omega* **2021**, *6*, 11813–11821.
[7] Z. Wu, N. Liu, W. Zheng, J. Chen, X. Song, J. Wang, C. Cui, D. Zhang, F. Zhao, *Propellants Explos. Pyrotech.* **2020**, *45*, 92–100.
[8] J. Zhang, B. B. Xue, G. N. Rao, L. P. Chen, W. H. Chen, *J. Therm. Anal. Calorim.* **2018**, 727–735.
[9] A. Książczak, M. Ostrowski, W. Tomaszewski, *J. Therm. Anal. Calorim.* **2008**, 275–279.
[10] F. Gao, B. Zhao, L. Hu, B. Chen, Y. Pan, P. Li, Y. Wang, *J. Chem. Eng. Data* **2020**, *65*, 3216–3220.
[11] P. Kočovský, *Tetrahedron Lett.* **1986**, 5521–5524.
[12] D. Trache, A. F. Tarchoun, *J. Mater. Sci.* **2018**, *53*, 100–123.
[13] Q. J. Axthammer, T. M. Klapötke, B. Krumm, *Z. Anorg. Allg. Chem.* **2016**, *642*, 211–218.
[14] A. L. J. Thiele, *Justus Liebigs Ann. Chem.* **1895**, *288*, 267–311.
[15] a) Q. J. Axthammer, T. M. Klapötke, B. Krumm, *Chem. Asian J.* **2016**, *11*, 568–575; b) Q. J. Axthammer, PhD Thesis, LMU Munich **2016**; c) Q. J. Axthammer, B. Krumm, T. M. Klapötke, *J. Org. Chem.* **2015**, *80*, 6329–6335.
[16] a) G. Gattow, W. K. Knoth, *Z. Anorg. Allg. Chem.* **1983**, *499*, 194–204; b) H. M. Curry, J. P. Mason, *J. Am. Chem. Soc.* **1951**, *73*, 5043–5046.
[17] W. Li, W. Feng, J. Hao, Z. Gao, L. Chen, W. Chen, *Org. Process Res. Dev.* **2019**, *23*, 2388–2393.
[18] G. Zhao, D. Kumar, P. Yin, C. He, G. H. Imler, D. A. Parrish, J. M. Shreeve, *Org. Lett.* **2019**, *21*, 1073–1077.
[19] D. Fischer, T. M. Klapötke, J. Stierstorfer, *Angew. Chem. Int. Ed.* **2014**, *53*, 8172–8175; *Angew. Chem.* **2014**, *126*, 8311–8314.
[20] W. J. Chute, G. E. Dunn, J. C. MacKenzie, G. S. Myers, G. N. R. Smart, J. W. Suggit, G. F. Wright, *Can. J. Res. Sect. B* **1948**, *26*, 114–137.
[21] G. E. Dunn, J. C. MacKenzie, G. F. Wright, *Can. J. Res.* **1948**, *26b*, 104–113.
[22] D. E. Chavez, M. A. Hiskey, D. L. Naud, D. Parrish, *Angew. Chem. Int. Ed.* **2008**, *47*, 8307–8309; *Angew. Chem.* **2008**, *120*, 8431–8433.
[23] a) L. Zhai, X. Qu, B. Wang, F. Bi, S. Chen, X. Fan, G. Xie, Q. Wei, S. Gao, *ChemPlusChem* **2016**, *81*, 1156–1159; b) Y. Liu, J. Zhang, K. Wang, J. Li, Q. Zhang, J. M. Shreeve, *Angew. Chem. Int. Ed.* **2016**, *55*, 11548–11551; *Angew. Chem.* **2016**, *128*, 11720–11723.
[24] J. Zhou, L. Ding, X. Wang, Y. Zhu, B. Wang, J. Zhang, *ChemistryOpen* **2018**, *7*, 527–532.
[25] N. Dai, A. D. Shah, L. Hu, M. J. Plewa, B. McKague, W. A. Mitch, *Environ. Sci. Technol.* **2012**, *46*, 9793–9801.
[26] R. G. Pews, *J. Org. Chem.* **1967**, *32*, 2914–2915.
[27] Impact: insensitive > 40 J, less sensitive ≥ 35 J, sensitive ≥ 4 J, very sensitive ≤ 3 J, Friction: insensitive > 360 N, less sensitive = 360 N, sensitive < 360 N and > 80 N, very sensitive ≤ 80 N, extremely sensitive ≤ 10 N. According to the UN Recommendations on the Transport of Dangerous Goods, (+) indicates not safe for transport.
[28] M. Sućeska, EXPLO5V6.06.01, Zagreb (Croatia), **2021**.

Submitted: June 10, 2022
Accepted: July 4, 2022